REACTION OF THE HALO NUCLEUS ^{11}Be ON HEAVY TARGETS AT ENERGIES AROUND THE COULOMB BARRIER*

V. Pesudo[a], M.J.G. Borge[a], A.M. Moro[b], E. Nacher[a], L. Acosta[c]
M. Alcorta[j], M.A.G. Alvarez[b,p], G.C. Ball[g], P.C. Bender[g], R. Braid[i]
M. Cubero[a,f], A. di Pietro[e], J.P. Fernandez-Garcia[b,d,k], P. Figuera[e]
M. Fisichella[e], B.R. Fulton[h], A.B. Garnsworthy[g]
J. Gomez-Camacho[b,d], G. Hackman[g], O.S. Kirsebom[g], K. Kuhn[i]
R. Krücken[g,s], M. Lattuada[e,o], J.A. Lay[l,m], G. Marquínez-Durán[c]
I. Martel[c], D. Miller[g], M. Moukaddam[g], P.D. O'Malley[i], A. Perea[a]
M.M. Rajabali[g], A.M. Sánchez-Benítez[c,n], F. Sarazin[i], V. Scuderi[e]
C.E. Svensson[r], O. Tengblad[a], C. Unsworth[g], Z.M. Wang[g,q]

[a]Instituto de Estructura de la Materia, CSIC, 28006 Madrid, Spain
[b]Dept. de Física Atómica, Molecular y Nucl., Univ. de Sevilla, 41080 Sevilla, Spain
[c]Departamento de Física Aplicada, Universidad de Huelva, 21071 Huelva, Spain
[d]CN de Aceleradores (U. Sevilla, J. Andalucía, CSIC), 41092, Sevilla, Spain
[e]Laboratori Nazionali del Sud, INFN, via Santa Sofia 62, 95123, Catania, Italy
[f]CICANUM, Universidad de Costa Rica, Apdo. 2060, San José, Costa Rica
[g]TRIUMF, 4004 Wesbrook Mall, Vancouver, British Columbia V6T 2A3, Canada
[h]Department of Physics, University of York, YO 10 5DD Heslington, York, UK
[i]Physics Department, Colorado School of Mines, Golden, Colorado 80401, USA
[j]Physics Division, Argonne National Laboratory, Argonne, Illinois 60439, USA
[k]Dept. de Física Atóm., Mol. y Nuclear, Univ. de Granada, 18071 Granada, Spain
[l]Dipart. di Fisica e Astr. "Galileo Galilei", Univ. di Padova, 35131 Padova, Italy
[m]INFN, Sezione di Padova, via Marzolo, 8, 35131 Padova, Italy
[n]GANIL, CEA/DSM-IN2P3-CNRS, B.P. 5027, 14076 Caen cedex, France
[o]Dipart. di Fisica e Astronomia, via Santa Sofia 64, 95123, Catania, Italy
[p]Instituto de Física, Universidade de São Paulo, 66318, São Paulo, Brazil
[q]Dept. of Chemistry, Simon Fraser University, Burnaby, BC, V5A 1S6, Canada
[r]Dept. of Physics. University of Guelph, Guelph, Ontario N1G 2W1, Canada
[s]Dept. of Physics, Univ. of British Columbia, Vancouver, BC, V6T 1Z1, Canada

(Received November 19, 2013)

New data for the reaction ^{11}Be on ^{197}Au at $E_{\rm lab} = 31.9$ MeV are presented. The angular distributions of the inelastically scattered ^{11}Be and the ^{10}Be fragments coming from the ^{11}Be dissociation have been extracted and compared with semiclassical and coupled-channels calculations in an angular range $\theta_{\rm lab} = 13°$–$46°$ for the detected Be fragment.

DOI:10.5506/APhysPolB.45.375
PACS numbers: 29.38.–c, 25.45.–De, 25.40.–Hs

* Presented at the XXXIII Mazurian Lakes Conference on Physics, Piaski, Poland, September 1–7, 2013.

1. Introduction

^{11}Be is a one-neutron halo nucleus ($J^\pi = 1/2^+$) and is one of the rare cases of halo nucleus with a bound excited state ($J^\pi = 1/2^-$). The neutron separation energy from the ground state is $S_n = 501.6$ keV [1]. The bound state, at 320.04(10) keV [1], has one of the largest known dipole transition strength between bound states ($B(\mathrm{E1}) = 0.116(12)\, e^2\mathrm{fm}^2$ [2]). Both excitation and dissociation can occur at low energies. Studying the scattering of this nucleus on heavy targets at energies around the Coulomb barrier is an excellent frame to understand how the halo structure influences the dynamics.

We present here preliminary ^{11}Be on ^{197}Au inelastic scattering and break-up cross sections, relative to elastic cross sections, for small scattering angles and energy of $E_{\mathrm{lab}} = 31.9$ MeV. We show that the first-order semiclassical Coulomb excitation theory [3] (or its interpretation as the Equivalent Photon Method, EPM) is appropriate to describe the inelastic scattering in this energy range, but underestimates the break-up probability. We also compare the differential cross sections with Continuum-Discretized Coupled-Channels calculations (CDCC) considering an inert ^{10}Be core and a valence neutron. In this case, break-up is well reproduced but inelastic scattering is overestimated.

2. Experimental setup

The experiment was performed at TRIUMF/ISAC-II, Vancouver, Canada. The secondary ^{11}Be beam was produced by a primary 500 MeV 40 μA proton beam from TRIUMF main cyclotron impinging on a tantalum target. After ionization with TRILIS laser ion source, extraction and separation, the ^{11}Be was post-accelerated, obtaining a continuous beam. Two ^{11}Be beam energies were measured, $3.599(3)A$ MeV and $2.901(4)A$ MeV, which on a ^{197}Au target are around and below the Coulomb barrier (around 39 MeV), respectively. The intensity of the radioactive beam was around 10^5 ^{11}Be/s. With a 2 mm collimator at the target position the transmission was $\approx 90\%$, what means a FWHM of the beam spot (assuming a Gaussian spot) of 1.4 mm. A ^{12}C beam at $5A$ MeV was used to study Rutherford scattering, for fine detector positioning and for energy calibration, using a ^{239}Pu, ^{241}Am and ^{244}Cm triple-alpha source, as well.

The target thickness was $1.9\,\mu\mathrm{g/cm}^2$ and it was tilted at 15° for minimizing its shade on the detectors. Our detectors were fixed to a printed circuit board and fitted inside the SHARC reaction chamber. Around the chamber, we placed two of the three TIGRESS rings for gamma detection [4]. The three rings were at $\theta_{\mathrm{lab}} = 45°$, 90°, 135°. Due to the chamber geometry, the 45° one could not be used. The 90° ring had 8 clovers homogeneously

distributed around ϕ and the 135° one had 4. Each clover is formed by 4 Ge crystals. The acquisition trigger was set on the charged particles detectors. The setup inside the chamber consisted of 4 silicon telescopes, 3 of them had a 40 μm 16 × 16 Double Sided Silicon Strip Detector (DSSSD) in the front backed by a 0.5 mm Silicon single PAD detector. These ones were centered at 28°, 45° and 76° and distances to the target center were 80 mm, 60 mm and 80 mm, respectively, giving an angular resolution of 3°. The one at most backward angle (130°, 45 mm) had a 20 μm Single Sided Silicon Strip Detector (SSSSD) backed by a 300 μm DSSSD. The results presented here correspond only to the most forward detector which covers $\theta_{\text{lab}} = 13°–46°$. The calibrations for the silicon detectors were made pixel by pixel using a triple alpha source and the ^{12}C beam. P and N sides of the DSSSD were calibrated independently and each of them had a FWHM for the alpha sources of ≈ 40 keV. The FWHM of the energy difference between the two sides of the DSSSD for the same incoming particle is 43 keV. For a real event to be considered, the difference between the front and back signals was restricted to less than 100 keV. The calibration of the PAD detector was made considering the pixel in which the ^{12}C beam had hit the DSSSD, for taking into account the different dead layer each particle had to go through.

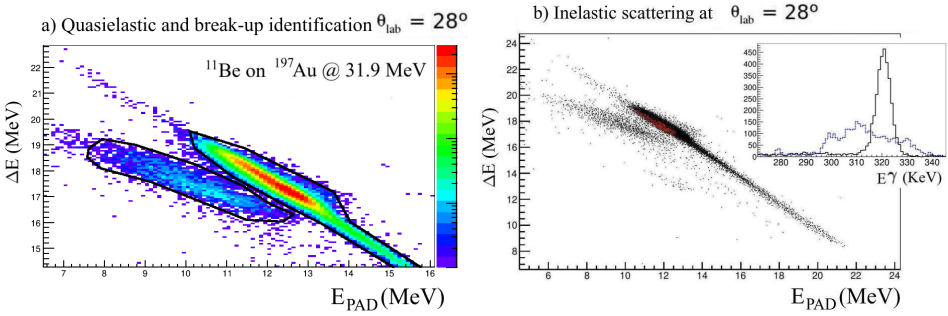

Fig. 1. (Color online) ^{11}Be on ^{197}Au at 31.9 MeV. (a) ΔE *versus* E_{back} plot showing the separation between quasielastic (namely elastic + inelastic) events and the ^{10}Be fragments after break-up, adding up all the pixels centered between 27° and 30°. (b) Full ΔE *versus* E_{back} plot, where particles in coincidence with a gamma at 320 keV are depicted in red. In the inset, the gamma spectrum in the region of interest is shown before (dashed/blue) and after Doppler correction (full line).

The total efficiency for gamma detection is 12.8% at 320 keV, which is the energy of the gamma produced in the desexcitation from the only bound excited state and the one we will gate on for the inelastic scattering study. This efficiency was calculated using a ^{60}Co source with a well known activity and a ^{152}Eu source for scaling to the low energy range, fitting to a Jäckel function [5]. The Doppler correction was made considering the

angle of particle detection and the angle of gamma detection event by event. The FWHM after Doppler correction of this peak is 7.0 keV. In Fig. 1 the two-dimensional plots of an angular bin, obtained with our high-granularity telescope configuration, are shown.

3. Results and discussion

Following our previous work on the ^{11}Li + ^{208}Pb reaction [6], for the analysis of the ^{10}Be production as resulting from break-up processes it is convenient to introduce the break-up probability. It is defined in this case as the ratio of outgoing ^{10}Be fragments with respect to the sum of elastic and non-elastic (break-up and inelastic) events for a given laboratory scattering angle. In a similar way, we define the inelastic probability as the ratio between the inelastic and the same sum (elastic and non-elastic events). We present the angular distribution of the break-up and inelastic scattering probability. Note that, for very small scattering angles, the elastic cross section should be close to the Rutherford one. As the scattering angle increases, the elastic cross section departs from the Rutherford due to higher order Coulomb couplings as well as nuclear effects. Energy losses in the target have been considered by assuming that the reaction takes place in the center of the target.

3.1. Analysis of the inclusive break-up

Since the experiment was inclusive with respect to the outgoing neutrons (only charged particles were detected), it cannot be assured that what we observe is direct break-up and not transfer to the continuum, but at the small angles presented here the contribution of the latter is expected to be small. Besides, the energy of the ^{10}Be is consistent with the one expected for direct break-up.

Given the large $B(\mathrm{E1})$ strength at low excitation energies [7–9], we also expect a dominance of the dipole Coulomb couplings in this experiment. Under this situation, the Alder and Winther semiclassical first-order Coulomb theory gives a break-up probability for a pure dipole excitation as

$$P_{bu}(\theta) = \left(\frac{Z_t e}{a_0 \hbar v}\right)^2 \frac{2\pi}{9} \int_{\varepsilon_b}^{\infty} d\varepsilon \frac{dB(\mathrm{E1},\varepsilon)}{d\varepsilon} \left(I^2_{1-1}(\theta,\varepsilon) + I^2_{11}(\theta,\varepsilon)\right) , \qquad (1)$$

$I^2_{1\pm1}(\theta,\varepsilon)$ being the Coulomb integrals [3].

For these calculations, we use a potential from the work of Capel *et al.* [10]. The $B(\mathrm{E1})$ distribution extracted with this potential sits between the one observed by Nakamura [8] and Fukuda [7] (which are compatible) and

the one observed by Palit [9]. The break-up probability calculated with this model is compared in Fig. 2 (a) with the data (dashed line). With this B(E1) distribution, the calculation underestimates the observed break-up probability. Since this calculation accounts only for the direct Coulomb break-up caused by the strong dipole polarization of the core-neutron system, we conclude that there are additional contributions to the break-up probability besides the direct E1 mechanism.

We have also compared the data with continuum-discretized coupled-channels (CDCC) calculations [11]. For these calculations, we have used a core-target potential from [12] for ^{10}Be on ^{208}Pb, due to the lack of data in ^{10}Be on ^{197}Au in this energy range. For the n–^{197}Au interaction, we use use the global parametrization of Koning and Delaroche [13]. Continuum states

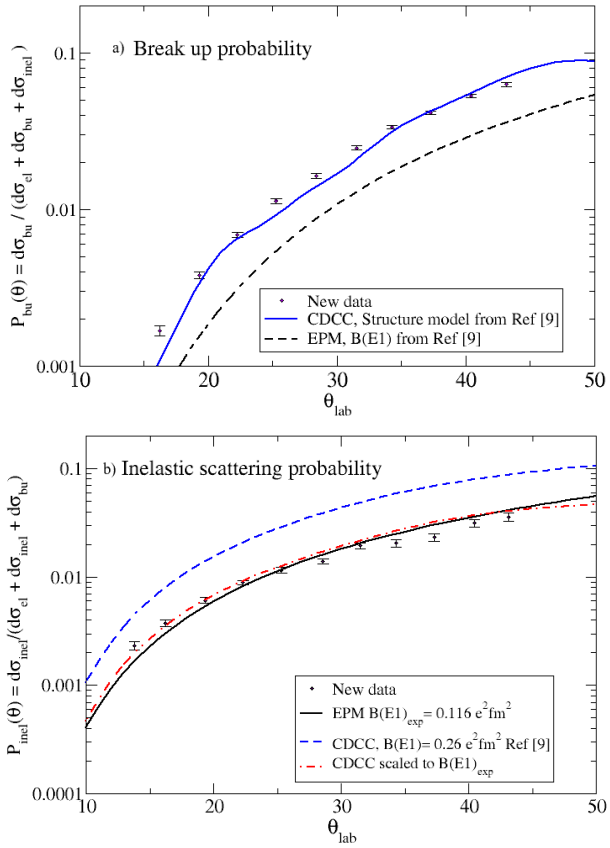

Fig. 2. New data from the ^{11}Be on ^{197}Au at 31.9 MeV (below the Coulomb barrier) compared to calculations (see the text for details). (a) Breakup probability; (b) Inelastic scattering probability for the excitation to the bound excited state at $E_x = 320$ keV.

are included for $\ell = 0, 1$ and 2 waves, and up to a maximum excitation energy of 5 MeV. For each (ℓ, s, j) configuration of the neutron relative to the ^{10}Be core, the continuum was discretized in momentum bins, following the standard average method. The calculations were performed with the code Fresco [14] and shows a good agreement with the experiment. The main contribution to the break-up probability arises from the $s_{1/2}$, $p_{1/2}$ and $p_{3/2}$ continuum states. The $p_{1/2}$ and $p_{3/2}$ states are mainly populated by a direct E1 mechanism, whereas the $s_{1/2}$ contribution comes mainly from two-step E1 mechanism going through the $p_{1/2}$ and $p_{3/2}$ states.

3.2. Analysis of inelastic cross section

In figure 2 (b), the inelastic scattering probability is compared with semiclassical and coupled channels calculations. Since the B(E1) for this transition is well known (B(E1) = 0.116(12) e^2fm^2 [2]), we use this value for the EPM calculation. Target absorption and anisotropy effects due to the multipolarity of the gamma transition are not considered here for the extraction of the experimental inelastic probability. We see that these calculations explain satisfactorily the data.

Our CDCC calculation reproduces the experimental break-up cross section, but overestimates the inelastic scattering cross section. This is not unexpected, since the adopted potential model (extracted from [10]) reproduces well the B(E1) distribution to the continuum, but overestimates the B(E1) to the bound excited state (B(E1) = 0.261 e^2fm^2, *i.e.* approximately twice the experimental value). This fact can be understood since, in this two-body model, the states of ^{11}Be are given by pure single-particle configurations of the valence neutron relative to an inert ^{10}Be(0$^+$) core. Thus, the ground state and first excited states correspond to pure $2s_{1/2}$ and $1p_{1/2}$ configurations, respectively. In a more realistic description, the states of ^{11}Be contain significant admixtures of excited states of the ^{10}Be core. So, for example, considering the 2$^+$ excited state of the core, we have

$$\begin{aligned}
\left|^{11}\mathrm{Be(g.s.)}\right\rangle_{1/2^+} &= \alpha \left|^{10}\mathrm{Be}(0^+) \otimes \nu(2s_{1/2})\right\rangle_{1/2^+} \\
&\quad + \beta \left|^{10}\mathrm{Be}(2^+) \otimes \nu(1d_{5/2})\right\rangle_{1/2^+} + \ldots \\
\left|^{11}\mathrm{Be}^*\right\rangle_{1/2^-} &= \alpha' \left|^{10}\mathrm{Be}(0^+) \otimes \nu(1p_{1/2})\right\rangle_{1/2^-} \\
&\quad + \beta' \left|^{10}\mathrm{Be}(2^+) \otimes \nu(1p_{3/2})\right\rangle_{1/2^-} + \ldots
\end{aligned}$$

Scaling the calculations by a factor of $B(\mathrm{E1})_{\mathrm{exp}}/B(\mathrm{E1})_{\mathrm{Capel}} = 0.116/0.261$, the coupled channels calculation matches the data and the semiclassical model.

4. Conclusions and outlook

We have presented new data for the inelastic and break-up probability angular distributions measured for the ^{11}Be + ^{197}Au reaction at an incident energy of 31.9 MeV, which is below the Coulomb barrier. A remarkably large yield of ^{10}Be has been observed for the angular range of $\theta_{\rm lab} = 13°$–$46°$. Semi-classical calculations, based in the first-order theory of Alder and Winther, underestimated the data. CDCC calculations, based on the same structure model of ^{11}Be, succeed in reproducing this observable and confirm the importance of higher order dipole Coulomb couplings to account for the data. On the other hand, the inelastic data measured in the same angular range are well described by the EPM calculations, provided that the experimental B(E1) value for this transition is used. The present CDCC calculations overestimated the data, a result that can be traced back to the fact that the potential model used in these calculations overestimates the experimental $B(\mathrm{E1}; 1/2^+ \to 1/2^-)$ value. In fact, scaling the CDCC result by the ratio of the experimental to model B(E1) values, the data is well reproduced.

These results evidence a need of a more sophisticated model to reproduce all the observables. Currently, some progress is being made to extend the CDCC formalism in order to incorporate core excitation effects in the structure of the ^{11}Be projectile as well as in the core–target interaction [15, 16]. A comparison of the data from this experiment with these extended CDCC calculations is in progress and will be presented in a future publication.

The analysis of the experimental data is being completed in order to include uncertainties in the scattering angles, and data analysis is being extended to larger angles (up to $\theta_{\rm lab} = 140°$). The extraction of the absolute values for the elastic cross section, and anisotropy effects in the desexcitation after inelastic scattering are under study.

This work was supported by the Spanish Government under the projects FPA2009-07387, FPA2009-07653, FPA2009-08848, FPA2012-32443 and Consolider CPAN CSD2007-00042; the Helmholtz Association (HGT) through the Nuclear Astrophysics Virtual Institute (VH-VI-417); ATI Sistemas; a Natural Sciences and Engineering Research Council of Canada grant. TRIUMF receives federal funding via a contribution agreement through the National Research Council of Canada.

REFERENCES

[1] J.H. Kelley *et al.*, *Nucl. Phys.* **A880**, 88 (2012).
[2] D.J. Millener *et al.*, *Phys. Rev.* **C28**, 497 (1983).

[3] K. Alder, A. Winther, *Electromagnetic Excitation*, North Holland, Amsterdam 1975.
[4] G.C. Ball *et al.*, *Nucl. Phys.* **A787**, 118c (2007).
[5] B. Jäckel *et al.*, *Nucl. Instrum. Methods* **A261**, 547 (1987).
[6] J.P. Fernandez-Garcia *et al.*, *Phys. Rev. Lett.* **110**, 142701 (2013).
[7] N. Fukuda *et al.*, *Phys. Rev.* **C70**, 054606 (2004).
[8] T. Nakamura *et al.*, *Phys. Rev. Lett.* **83**, 1112 (1994).
[9] R. Palit *et al.*, *Phys. Rev.* **C68**, 034318 (2003).
[10] P. Capel *et al.*, *Phys. Rev.* **C70**, 064605 (2004).
[11] N. Austern *et al.*, *Phys. Rep.* **153**, 125 (1987).
[12] J.J. Kolata *et al.*, *Phys. Rev.* **C69**, 047601 (2007).
[13] A.J. Koning, J.P. Delaroche, *Nucl. Phys.* **A713**, 231 (2003).
[14] I.J. Thompson, *Comput. Phys. Rep.* **7**, 167 (1988).
[15] N.C. Summers *et al.*, *Phys. Lett.* **B650**, 124 (2007).
[16] J.A. Lay *et al.*, *AIP Conf. Proc.* **1488**, 436 (2012).